December 2005

# Decoherence modes of entangled qubits within neutron interferometry

Reinhold A. Bertlmann,[1] Katharina Durstberger,[1,*] and Yuji Hasegawa[2,3]

[1] *Institute for Theoretical Physics, University of Vienna*
*Boltzmanngasse 5, 1090 Vienna, Austria*
[2] *Atominstitut der Österreichischen Universitäten*
*Stadionallee 2, 1020 Vienna, Austria*
[3] *PRESTO, Japan Science and Technology Agency*
*4-1-8 Honcho Kawaguchi, Saitama, Japan*

arXiv:quant-ph/0512103v1 13 Dec 2005

We study two different decoherence modes for entangled qubits by considering a Liouville – von Neumann master equation. Mode A is determined by projection operators onto the eigenstates of the Hamiltonian and mode B by projectors onto rotated states. We present solutions for general and for Bell diagonal states and calculate for the later the mixedness and the amount of entanglement given by the concurrence.

We propose a realization of the decoherence modes within neutron interferometry by applying fluctuating magnetic fields. An experimental test of the Kraus operator decomposition describing the evolution of the system for each mode is presented.

PACS numbers: 03.65.Yz, 03.75.Dg, 42.50.-p

Keywords: Entanglement, decoherence, master equation, Kraus operators, Bell diagonal states, neutron interferometry

## I. INTRODUCTION

Closed quantum systems are idealizations which do not exist in a real physical world. Actually, one always has to deal with open quantum systems which arise due to an interaction of the system under consideration with an external environment (e.g. reservoir, heat bath) [1, 2, 3]. The system – environment interaction causes a phenomenon known as decoherence: quantum correlations and interferences are destroyed in course of time; the system shows more and more classical behavior. The theory of decoherence is one candidate to solve the question why our world looks so classical [3, 4].

The total Hamiltonian of system and environment generates a unitary time evolution $U(t)$ and is of the form $H_{SE} = H \otimes \mathbb{1}_E + \mathbb{1} \otimes H_E + H_I$, where $H$, $H_E$ and $H_I$ are, respectively, the system, environment and interaction Hamiltonians. The evolution of the system,

*Electronic address: katharina.durstberger@univie.ac.at

represented by the density matrix $\rho(t)$, or the reduced dynamics is obtained by tracing over the environmental degrees of freedom $\rho(t) = \mathrm{Tr}_E\, \rho_{S+E}(t) = \mathrm{Tr}_E(U(t)\rho_{S+E}(0)U^\dagger(t))$ and thus inheriting a nonunitary evolution for the system in contrast to closed systems.

In most of the cases we do not have access or information about the dynamics of the environment. Therefore we have to describe the evolution of the system by an effective dynamics: the Liouville – von Neumann master equation. Thereby it is not so important to know the exact Hamiltonian and the nature of the environment but only its effects on the system. Our strategy in this paper is to propose several effective models which do not care about the exact nature of decoherence but provide scenarios how decoherence can affect a system.

Under several assumptions [1], such as Markovian semigroup approach, complete positivity, initial decoupling of system and environment, and weak coupling, the dynamics of the system can be described by a Liouville – von Neumann master equation

$$\frac{\partial}{\partial t}\rho(t) = -i[H(t), \rho(t)] - D[\rho(t)] \; . \tag{1}$$

Lindblad and Gorini–Kossakowski–Sudarshan [5, 6] derived the most general structure of the dissipator

$$D[\rho(t)] = \frac{1}{2}\sum_k \big(A_k^\dagger A_k \rho(t) + \rho(t) A_k^\dagger A_k - 2A_k\rho(t)A_k^\dagger\big) \; , \tag{2}$$

where $A_k$ represents a so-called Lindblad generator. The sum is taken over an arbitrary number of components but maximally up to $n^2-1$, where $n$ denotes the dimension of the system. For simplicity we choose the generators to be projectors such that $A_k = \sqrt{\lambda_k}P_k$ with $P_k^2 = P_k$ (see Ref.[7]) which gives for the dissipator

$$D[\rho] = \frac{1}{2}\sum_k \lambda_k\big(P_k\rho + \rho P_k - 2P_k\rho P_k\big) \; . \tag{3}$$

The paper is organized as follows. In the next section we introduce and discuss two possible decoherence scenarios for a two qubit system by choosing different projection operators $P_k$. In Sect.III the two decoherence modes are discussed for the special case of Bell diagonal states. In Sect.IV we propose a realization of the decoherence modes within neutron interferometry via random magnetic fields which represent the environment. In Sect.V we present the Kraus operator decomposition. The action of this decomposition is mathematically equivalent to the Lindblad form of the Liouville – von Neumann equation. We can test this equivalence by a simple experiment with single neutrons.

## II. DECOHERENCE MODES IN A TWO QUBIT SYSTEM

Let us consider a two qubit system with Hilbertspace $\mathcal{H} = \mathcal{H}^{(1)} \otimes \mathcal{H}^{(2)} = \mathbb{C}^2 \otimes \mathbb{C}^2$ where $\{|e_k\rangle\}_{k=1,\ldots,4}$ denotes an eigenbasis defined by $H|e_k\rangle = E_k|e_k\rangle$, with $H = H^{(1)}\otimes\mathbb{1} + \mathbb{1}\otimes H^{(2)}$ the Hamiltonian of the undisturbed system. A general state $\rho$ of the system can be

expressed in the eigenbasis $\rho = \sum_{k,j} \rho_{kj} |e_k\rangle\langle e_j|$, where $(\rho_{kj})$ denotes the $4 \times 4$ coefficient matrix.

We consider Lindblad generators $P_k$ that project onto one-dimensional subspaces and fulfil $\sum_k P_k = \mathbb{1}$, furthermore we assume that only one dissipation parameter $\lambda$ parameterizes the strength of the interaction and therefore of the decoherence. Then the dissipator, Eq.(3), can be written as

$$D[\rho] = \lambda\big(\rho - \sum_{k=1}^{4} P_k \rho P_k\big) \ . \tag{4}$$

In the following sections we solve the Liouville – von Neumann equation (1) with the dissipator (4) by assuming different projection operators $P_k$, what we call decoherence modes.

### A. Mode A

The first mode describes the simplest possible case. The Lindblad generators are chosen to be projectors $P_k = |e_k\rangle\langle e_k|$ onto the eigenbasis of the Hamiltonian (see Refs.[8, 9]). In this mode of decoherence the time evolution (1) for the coefficient matrix is given by

$$\begin{aligned} \dot{\rho_{kj}} &= \big(-i(E_k - E_j) - \lambda_A\big)\rho_{kj} \qquad \text{for } k \neq j \\ \dot{\rho_{kk}} &= 0 \ , \end{aligned} \tag{5}$$

which can be easily solved

$$\begin{aligned} \rho_{kj}(t) &= e^{-i(E_k - E_j)t} e^{-\lambda_A t} \rho_{kj}(0) \qquad \text{for } k \neq j \\ \rho_{kk}(t) &= \rho_{kk}(0) \ . \end{aligned} \tag{6}$$

The decoherence affects only the off-diagonal elements and leaves the diagonal elements untouched.

### B. Mode B

For the second mode the Lindblad generators are chosen to be projectors $\widetilde{P_k} = |\widetilde{e_k}\rangle\langle\widetilde{e_k}|$ onto the following states

$$|\widetilde{e_{1,3}}\rangle = \frac{1}{\sqrt{2}}(|e_1\rangle \pm |e_3\rangle) \ , \qquad\qquad |\widetilde{e_{2,4}}\rangle = \frac{1}{\sqrt{2}}(|e_2\rangle \pm |e_4\rangle) \ , \tag{7}$$

where the upper (lower) sign corresponds to the first (second) index.

The time evolution (1) of the coefficient matrix can be separated into 3 types of differential equations. Type I is valid for the components $\rho_{12}, \rho_{14}, \rho_{23}, \rho_{34}$ and has the structure

$$\dot{\rho_{12}} = \big(-i(E_1 - E_2) - \lambda_B\big)\rho_{12} \ , \tag{8}$$

in analogy to mode A. Type II holds for the diagonal components and reveals pairwise coupled differential equations for $\rho_{11} - \rho_{33}$ and $\rho_{22} - \rho_{44}$ of the form

$$\dot{\rho_{11}} = -\frac{\lambda_B}{2}\rho_{11} + \frac{\lambda_B}{2}\rho_{33} \ , \qquad \dot{\rho_{33}} = \frac{\lambda_B}{2}\rho_{11} - \frac{\lambda_B}{2}\rho_{33} \ . \tag{9}$$

Type III also gives pairwise coupled differential equations

$$\dot{\rho_{13}} = \big(-i(E_1 - E_3) - \frac{\lambda_B}{2}\big)\rho_{13} + \frac{\lambda_B}{2}\rho_{31} \ , \qquad \dot{\rho_{31}} = \frac{\lambda_B}{2}\rho_{13} + \big(i(E_1 - E_3) - \frac{\lambda_B}{2}\big)\rho_{31} \ , \tag{10}$$

valid for the components $\rho_{13} - \rho_{31}$ and $\rho_{24} - \rho_{42}$. The solutions for the several types of differential equations are:
for type I, Eq.(8),

$$\rho_{12}(t) = e^{-i(E_1 - E_2)t} e^{-\lambda_B t} \rho_{12}(0) \ , \tag{11}$$

for type II, Eq.(9),

$$\begin{aligned} \rho_{11}(t) &= \frac{1}{2}(1 + e^{-\lambda_B t})\rho_{11}(0) + \frac{1}{2}(1 - e^{-\lambda_B t})\rho_{33}(0) \ , \\ \rho_{33}(t) &= \frac{1}{2}(1 - e^{-\lambda_B t})\rho_{11}(0) + \frac{1}{2}(1 + e^{-\lambda_B t})\rho_{33}(0) \ , \end{aligned} \tag{12}$$

for type III, Eq.(10),

$$\begin{aligned} \rho_{13}(t) &= e^{-\frac{\lambda_B t}{2}} \left( \Big( \cosh \frac{\mu t}{2} - \frac{2i(E_1 - E_3)}{\mu} \sinh \frac{\mu t}{2} \Big) \rho_{13}(0) + \frac{\lambda_B}{\mu} \sinh \frac{\mu t}{2} \rho_{31}(0) \right) \ , \\ \rho_{31}(t) &= e^{-\frac{\lambda_B t}{2}} \left( \Big( \cosh \frac{\mu t}{2} + \frac{2i(E_1 - E_3)}{\mu} \sinh \frac{\mu t}{2} \Big) \rho_{31}(0) + \frac{\lambda_B}{\mu} \sinh \frac{\mu t}{2} \rho_{13}(0) \right) \ , \end{aligned} \tag{13}$$

where $\mu = \sqrt{\lambda_B^2 - 4(E_1 - E_3)^2}$.

Decoherence mode B affects not only the off-diagonal elements of the density matrix but also the diagonal ones.

In the case we consider in this paper – decoherence modes in neutron interferometry, Sect.IV – the system is given by the free neutron passing through the interferometer, whereas the magnetic fields placed in represent the external environment. Thus there is no splitting in the energies, e.g., $E_1 = E_3$, $E_2 = E_4$ and $\mu = \lambda_B$, so that type III is equal to type II.

*Remark.* It is worth noting here that the choice of projection states, Eq.(7), corresponds to a rotation of states in one subspace. Suppose we split the eigenstates of the undisturbed Hamiltonian in eigenstates of the subspace Hamiltonians $\{|a_1\rangle, |a_2\rangle\}$ and $\{|b_1\rangle, |b_2\rangle\}$ in the following way

$$|e_{1,3}\rangle = |a_{1,2}\rangle|b_1\rangle \ , \qquad |e_{2,4}\rangle = |a_{1,2}\rangle|b_2\rangle \ . \tag{14}$$

Now consider a rotation of the first subbasis, $\{|+\rangle = \frac{1}{\sqrt{2}}(|a_1\rangle + |a_2\rangle), |-\rangle = \frac{1}{\sqrt{2}}(|a_1\rangle - |a_2\rangle)\}$, the second subbasis is left untouched. The basis of the total Hilbertspace changes

$$\begin{aligned} |\widetilde{e_1}\rangle &= |+\rangle|b_1\rangle = \frac{1}{\sqrt{2}}(|e_1\rangle + |e_3\rangle) \,, & |\widetilde{e_2}\rangle &= |+\rangle|b_2\rangle = \frac{1}{\sqrt{2}}(|e_2\rangle + |e_4\rangle) \,, \\ |\widetilde{e_3}\rangle &= |-\rangle|b_1\rangle = \frac{1}{\sqrt{2}}(|e_1\rangle - |e_3\rangle) \,, & |\widetilde{e_4}\rangle &= |-\rangle|b_2\rangle = \frac{1}{\sqrt{2}}(|e_2\rangle - |e_4\rangle) \,, \end{aligned} \tag{15}$$

which corresponds exactly to the states used in Eq.(7). Therefore decoherence mode B can be denoted "$R \otimes E$" to indicate the rotation of the first subspace and the untouched eigenbasis in the second subspace whereas mode A can be labelled by "$E \otimes E$".

In the case of photons (see, e.g., [10]) the eigenbasis $E$ corresponds to horizontal $|H\rangle$ and vertical $|V\rangle$ polarization whereas the rotated basis $R$ represents polarization states $|+45°\rangle$ and $|-45°\rangle$. In the case of neutral kaons (for an overview see, e.g., [11, 12]) we can identify the eigenbasis $E$ with the short- and long-lived states $|K_S\rangle$ and $|K_L\rangle$ and the rotated basis $R$ with $|K^0\rangle$ and $|\bar{K}^0\rangle$.

## III. INITIAL CONDITIONS – BELL DIAGONAL STATES

We want to illustrate the above discussed decoherence modes by choosing a certain class of states as initial conditions – the so-called Bell diagonal states $\rho = \sum_i \nu_i |\Psi_i\rangle\langle\Psi_i|$ with $\sum_i \nu_i = 1$, which are diagonal in the Bell basis

$$|\Psi_{1,2}\rangle = \frac{1}{\sqrt{2}}(|e_1\rangle \pm |e_4\rangle) \,, \qquad |\Psi_{3,4}\rangle = \frac{1}{\sqrt{2}}(|e_2\rangle \pm |e_3\rangle) \,. \tag{16}$$

In the standard basis they are expressed by

$$\rho = \frac{1}{2}\begin{pmatrix} \nu_1+\nu_2 & 0 & 0 & \nu_1-\nu_2 \\ 0 & \nu_3+\nu_4 & \nu_3-\nu_4 & 0 \\ 0 & \nu_3-\nu_4 & \nu_3+\nu_4 & 0 \\ \nu_1-\nu_2 & 0 & 0 & \nu_1+\nu_2 \end{pmatrix} = \frac{1}{2}\begin{pmatrix} \Sigma_1 & 0 & 0 & \Delta_1 \\ 0 & \Sigma_2 & \Delta_2 & 0 \\ 0 & \Delta_2 & \Sigma_2 & 0 \\ \Delta_1 & 0 & 0 & \Sigma_1 \end{pmatrix} \,, \tag{17}$$

using the notation $\Sigma_1 = \nu_1 + \nu_2$, $\Sigma_2 = \nu_3 + \nu_4$, $\Delta_1 = \nu_1 - \nu_2$, $\Delta_2 = \nu_3 - \nu_4$.

States are characterized by two quantities: mixing and entanglement. The mixedness, defined as $\delta = \mathrm{Tr}\rho^2$, ranges between 1 (pure states) and $\frac{1}{4}$ (maximally mixed states) and is given by $\delta = \nu_1^2 + \nu_2^2 + \nu_3^2 + \nu_4^2$ for Bell diagonal states. The concurrence $C$ [13, 14, 15] is a suitable quantity that measures the entanglement contained in a state $\rho$. It is defined by $C(\rho) = \max\{0, \mu_1 - \mu_2 - \mu_3 - \mu_4\}$, where $\mu_i$ are the square roots of the eigenvalues in decreasing order of the matrix $R = \rho\,(\sigma_y \otimes \sigma_y)\,\rho^*\,(\sigma_y \otimes \sigma_y)$ and $\rho^*$ denotes complex conjugation in the standard basis. The concurrence varies between 1 (maximally entangled states) and 0 (separable states) and is given by $C = \max\big\{0, 2\max\{\nu_i\} - 1\big\}$ for Bell diagonal states, depending on which weight $\nu_i$ is the largest. A Bell diagonal state can only be entangled ($C > 0$) if the largest eigenvalue fulfills $\nu_i > \frac{1}{2}$.

The special case of a pure and maximally entangled Bell state, e.g., the Bell singlet state $|\Psi_4\rangle$, where $\nu_4 = 1$ and $\nu_1 = \nu_2 = \nu_3 = 0$ or $\Sigma_1 = \Delta_1 = 0$ and $\Sigma_2 = -\Delta_2 = 1$, yields $\delta = 1$ and $C = 1$.

### A. Mode A

The initial Bell diagonal state, Eq.(17), evolves in time according to mode A, Eq.(6), into the state

$$\rho(t) = \frac{1}{2}\begin{pmatrix} \Sigma_1 & 0 & 0 & e^{-\lambda_A t}\Delta_1 \\ 0 & \Sigma_2 & e^{-\lambda_A t}\Delta_2 & 0 \\ 0 & e^{-\lambda_A t}\Delta_2 & \Sigma_2 & 0 \\ e^{-\lambda_A t}\Delta_1 & 0 & 0 & \Sigma_1 \end{pmatrix} . \tag{18}$$

For the mixedness of the state we get $\delta = \frac{1}{2}\big(\Sigma_1^2 + \Sigma_2^2 + e^{-2\lambda_A t}(\Delta_1^2 + \Delta_2^2)\big)$ and for the concurrence we find $C(\rho) = \max\big\{0, 2\max\{\mu_i\} - 1\big\}$, where $\mu_{1,2} = \frac{1}{2}(\Sigma_1 \pm e^{-\lambda_A t}\Delta_1)$ and $\mu_{3,4} = \frac{1}{2}(\Sigma_2 \pm e^{-\lambda_A t}\Delta_2)$.

Choosing the Bell singlet state $|\Psi_4\rangle$ the mixedness $\delta = \frac{1}{2}(1+e^{-2\lambda_A t})$ ranges from a pure state ($\delta = 1$) to a mixed but not maximally mixed state ($\delta \xrightarrow{t\to\infty} \frac{1}{2}$). The concurrence $C(\rho) = e^{-\lambda_A t}$ decreases exponentially from a maximally entangled state ($C = 1$) to an asymptotically separable state ($C \xrightarrow{t\to\infty} 0$). The behavior of $\delta$ and $C$ is plotted in Fig.1.

### B. Mode B

The second mode, Eqs.(11)-(13), generates the density matrix

$$\rho(t) = \frac{1}{4}\begin{pmatrix} 1 - e^{-\lambda_B t}\,\Delta & 0 & 0 & 2e^{-\lambda_B t}\Delta_1 \\ 0 & 1 + e^{-\lambda_B t}\,\Delta & 2e^{-\lambda_B t}\Delta_2 & 0 \\ 0 & 2e^{-\lambda_B t}\Delta_2 & 1 + e^{-\lambda_B t}\,\Delta & 0 \\ 2e^{-\lambda_B t}\Delta_1 & 0 & 0 & 1 - e^{-\lambda_B t}\,\Delta \end{pmatrix} , \tag{19}$$

with the notation $\Delta = \Sigma_1 - \Sigma_2$.

We obtain for the mixedness $\delta = \frac{1}{4}\Big(1 + e^{-2\lambda_B t}\big(2\Delta_1^2 + 2\Delta_2^2 + (\Sigma_1 + \Sigma_2)^2\big)\Big)$ and for the entanglement $C(\rho) = \max\big\{0, 2\max\{\mu_i\} - 1\big\}$, where $\mu_{1,2} = \frac{1}{4}(1 + e^{-\lambda_B t}(\Delta \pm 2\Delta_2))$ and $\mu_{3,4} = \frac{1}{4}(1 - e^{-\lambda_B t}(\Delta \mp 2\Delta_1))$.

The special case of $|\Psi_4\rangle$ yields the following results. The mixedness $\delta = \frac{1}{4}(1+3e^{-2\lambda_B t})$ varies from a pure state ($\delta = 1$) to a maximally mixed state ($\delta \xrightarrow{t\to\infty} \frac{1}{4}$). The concurrence $C(\rho) = \max\big\{0, \frac{1}{2}(3e^{-\lambda_B t} - 1)\big\}$ decreases exponentially and the initially maximally entangled state ($C = 1$) reaches the border of separability ($C = 0$) at finite time $t = \frac{\ln 3}{\lambda_B}$ where the mixing has the value of $\delta = \frac{1}{3}$ (see also Ref.[16]). In Fig.1 the dependence of $\delta$ and $C$ with respect to $\lambda t$ is shown.

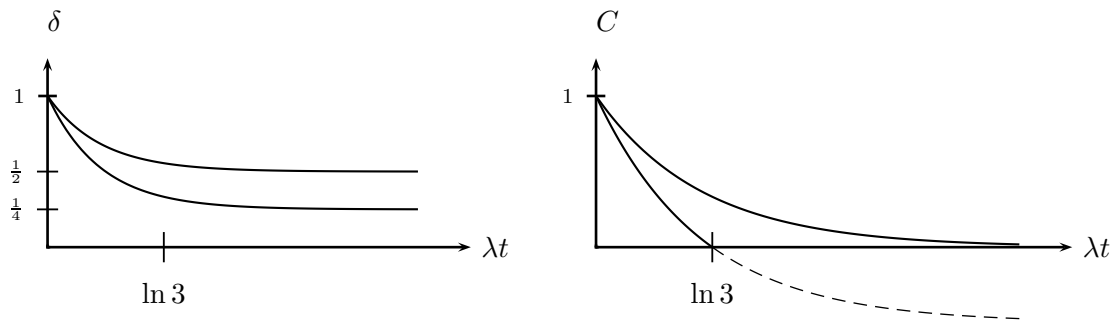


FIG. 1: Graphical comparison of the mixedness $\delta$ and the concurrence $C$ in dependence of $\lambda t$ for mode A and B for the Bell singlet state $|\Psi_4\rangle$. The upper curves correspond to mode A and the lower ones to mode B.

## IV. REALIZATION OF DECOHERENCE MODES FOR NEUTRON STATES

The different decoherence modes presented in Sect.II and discussed for Bell diagonal states in Sect.III can be tested within neutron interferometry [17]. A neutron is entangled [18, 19, 20] between the internal degree of freedom – spin – and the external degree of freedom – path – which is described by the bipartite Hilbertspace $\mathcal{H} = \mathcal{H}_{\text{spin}} \otimes \mathcal{H}_{\text{path}}$. Let us consider the antisymmetric Bell state which is experimentally feasible

$$|\Psi_{\text{exp}}\rangle \equiv |\Psi_4\rangle = \frac{1}{\sqrt{2}}(|\Uparrow\rangle \otimes |\text{II}\rangle - |\Downarrow\rangle \otimes |\text{I}\rangle) = \frac{1}{\sqrt{2}}(|e_2\rangle - |e_3\rangle) \ , \tag{20}$$

where $|\Uparrow\rangle$ and $|\Downarrow\rangle$ represent $\pm z$ polarized spin states whereas $|\text{I}\rangle$ and $|\text{II}\rangle$ denote the paths in the interferometer.

Calculating the density matrices for both modes A and B we find

$$\rho^A(t) = \frac{1}{2}\begin{pmatrix} 0 & 0 & 0 & 0 \\ 0 & 1 & -e^{-\lambda_A t} & 0 \\ 0 & -e^{-\lambda_A t} & 1 & 0 \\ 0 & 0 & 0 & 0 \end{pmatrix} \ , \tag{21}$$

$$\rho^B(t) = \frac{1}{4}\begin{pmatrix} 1-e^{-\lambda_B t} & 0 & 0 & 0 \\ 0 & 1+e^{-\lambda_B t} & -2e^{-\lambda_B t} & 0 \\ 0 & -2e^{-\lambda_B t} & 1+e^{-\lambda_B t} & 0 \\ 0 & 0 & 0 & 1-e^{-\lambda_B t} \end{pmatrix} \ . \tag{22}$$

The off-diagonal elements fade away exponentially for both modes. For mode B the diagonal elements are distributed in the whole 4-dimensional space so that at $t \to \infty$ the density matrix approaches the normed unity, i.e., the totally mixed state.

Within neutron interferometry all matrix elements can be determined experimentally [21] via the procedure of quantum state tomography [22].

### A. Decoherence via random magnetic fields

For the implementation of decoherence we use randomly fluctuating magnetic fields which act on an ensemble of neutrons produced in the specific state $\rho$.

The action of a magnetic field $\vec{B} = B\vec{n}$ in the direction $\vec{n}$ on a neutron state is described by the unitary operator $U(\alpha) = e^{i\frac{\alpha}{2}\vec{n}\cdot\vec{\sigma}}$, where $\alpha = 2\mu_B Bt = \omega_L t$ denotes the rotation angle and $\mu_B$, $\omega_L$ the Bohr magneton and Larmor frequency, respectively.

The neutron beam passes a fluctuating magnetic field in such a way that each neutron which is part of the quantum mechanical ensemble described by $\rho$ feels separately a different but constant magnetic field. This corresponds to applying a unitary operator $U(\alpha)$ with constant rotation angle $\alpha$ onto the density matrix $\rho$. For the whole ensemble we have to take the integral over all possible rotation angles $\alpha$

$$\rho \longrightarrow \rho' = \int \underbrace{U(\alpha)\,\rho\,U^\dagger(\alpha)}_{\rho(\alpha)}\; P(\alpha)d\alpha \;, \tag{23}$$

where $P(\alpha)$ denotes a distribution function. In our case the distribution function is a Gaussian $P(\alpha) = \frac{1}{\sqrt{2\pi}\sigma}e^{-\frac{\alpha^2}{2\sigma^2}}$ with standard deviation $\sigma$. Although each transformation separately is unitary due to the integration we end up with a nonunitary evolution.

### B. Mode A

For an incoming polarized neutron the state $|\Psi_{\text{exp}}\rangle$ is prepared after passing the beam splitter and spin flipper. This initial state is subjected to the fluctuating magnetic fields oriented along the $z$-axis in each path of the interferometer, see Fig.2. The rotations $U(\alpha)$ and $U(\beta)$ caused by the fields are independent but their distributions have the same deviation $\sigma$.

The action of the two magnetic fields can be described by a "conditioned operation". Depending on the state of the spatial degree of freedom either operation $U(\alpha)$ or $U(\beta)$ is applied to the spin state

$$\begin{aligned} |\psi_{\text{spin}}\rangle \otimes |\text{I}\rangle &\longrightarrow U(\alpha)|\psi_{\text{spin}}\rangle \otimes |\text{I}\rangle \\ |\psi_{\text{spin}}\rangle \otimes |\text{II}\rangle &\longrightarrow U(\beta)|\psi_{\text{spin}}\rangle \otimes |\text{II}\rangle \;. \end{aligned} \tag{24}$$

For a single neutron the application of the conditioned operation on the initial state $|\Psi_{\text{exp}}\rangle$, Eq.(20), gives

$$\rho(\alpha,\beta) = \frac{1}{2}\begin{pmatrix} 0 & 0 & 0 & 0 \\ 0 & 1 & -e^{i\frac{\alpha+\beta}{2}} & 0 \\ 0 & -e^{-i\frac{\alpha+\beta}{2}} & 1 & 0 \\ 0 & 0 & 0 & 0 \end{pmatrix} \;, \tag{25}$$

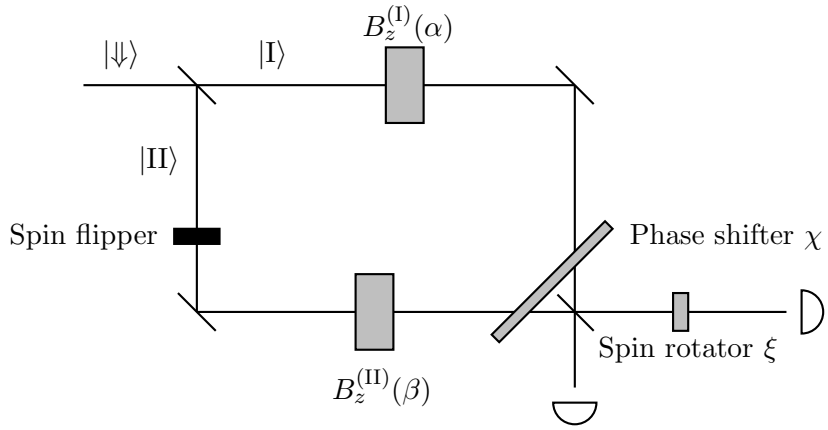


FIG. 2: Experimental setup for the realization of mode A. The spin flipper is inserted to achieve the Bell singlet state. The magnetic fields $B_z^{(\mathrm{I})}(\alpha)$ and $B_z^{(\mathrm{II})}(\beta)$ produce independent rotations $U(\alpha)$ and $U(\beta)$, respectively. With the phase shifter $\chi$ and the spin rotator $\xi$ the final state is analyzed.

which after integration over $\alpha$ and $\beta$ turns into

$$\rho' = \int \rho(\alpha,\beta)\, P(\alpha)\, P(\beta) d\alpha\, d\beta = \frac{1}{2}\begin{pmatrix} 0 & 0 & 0 & 0 \\ 0 & 1 & -e^{-\frac{\sigma^2}{4}} & 0 \\ 0 & -e^{-\frac{\sigma^2}{4}} & 1 & 0 \\ 0 & 0 & 0 & 0 \end{pmatrix} . \tag{26}$$

By comparison of Eq.(21) and Eq.(26) we immediately see that

$$\lambda_A t = \frac{\sigma^2}{4} , \tag{27}$$

the decoherence parameter $\lambda_A$ is directly related to the deviation $\sigma$ of the fluctuating magnetic fields. Note, that for only one magnetic field located in one of the paths fluctuating with deviation $\sigma$ the above relation is given by $\lambda_A t = \frac{\sigma^2}{8}$, and for one field acting on both paths we have $\lambda_A t = \frac{\sigma^2}{2}$.

### C. Mode B

For mode B we prepare the same state $|\Psi_{\mathrm{exp}}\rangle$ but use different fluctuating magnetic fields, shown in Fig.3. The different unitary operations caused by the magnetic fields are assumed to act independently but the Gaussian distributions have the same deviation $\sigma$.

In order to implement experimentally the rotated projectors (7) we need a magnetic field in $x$-direction $B_x$. However, to achieve the same damping in the off-diagonal elements as in the diagonal elements we have to insert an additional magnetic field in $z$-direction $B_z$ which influences only the off-diagonal elements. It reflects somehow the effect of the Kraus operators which act in $x$- and $z$-direction (see operator $M_3$ in Eq.(34)).

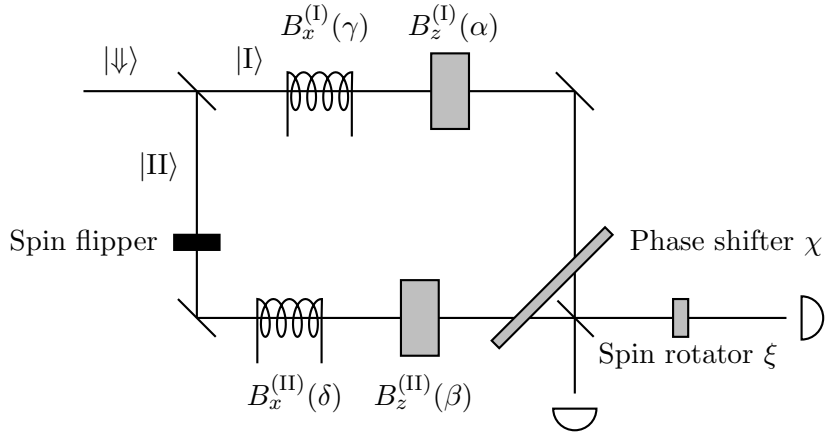


FIG. 3: Experimental setup for the realization of mode B. The magnetic fields $B_x^{(\mathrm{I})}(\gamma)$, $B_x^{(\mathrm{II})}(\delta)$, $B_z^{(\mathrm{I})}(\alpha)$ and $B_z^{(\mathrm{II})}(\beta)$ generate independent unitary rotations $U(\gamma)$, $U(\delta)$, $U(\alpha)$ and $U(\beta)$, respectively. The order of the magnetic fields in each path does not matter in this context.

The neutron after the conditioned operation is described by the density matrix

$$\rho(\alpha,\beta,\gamma,\delta) = \\ = \frac{1}{2}\begin{pmatrix} \sin^2\frac{\gamma}{2} & -i\sin\frac{\gamma}{2}\cos\frac{\delta}{2}e^{i\frac{\alpha-\beta}{2}} & \frac{1}{2}i\sin\gamma e^{i\alpha} & -\sin\frac{\gamma}{2}\sin\frac{\delta}{2}e^{i\frac{\alpha+\beta}{2}} \\ i\sin\frac{\gamma}{2}\cos\frac{\delta}{2}e^{-i\frac{\alpha-\beta}{2}} & \cos^2\frac{\delta}{2} & -\cos\frac{\gamma}{2}\cos\frac{\delta}{2}e^{i\frac{\alpha+\beta}{2}} & -\frac{1}{2}i\sin\delta e^{i\beta} \\ -\frac{1}{2}i\sin\gamma e^{-i\alpha} & -\cos\frac{\gamma}{2}\cos\frac{\delta}{2}e^{-i\frac{\alpha+\beta}{2}} & \cos^2\frac{\gamma}{2} & i\cos\frac{\gamma}{2}\sin\frac{\delta}{2}e^{-i\frac{\alpha-\beta}{2}} \\ -\sin\frac{\gamma}{2}\sin\frac{\delta}{2}e^{-i\frac{\alpha+\beta}{2}} & \frac{1}{2}i\sin\delta e^{-i\beta} & -i\cos\frac{\gamma}{2}\sin\frac{\delta}{2}e^{i\frac{\alpha-\beta}{2}} & \sin^2\frac{\delta}{2} \end{pmatrix}. \tag{28}$$

For the ensemble state we get after the integrations over the angles $\alpha$, $\beta$, $\gamma$, $\delta$ with Gaussian weights

$$\rho' = \frac{1}{4}\begin{pmatrix} 1-e^{-\frac{\sigma^2}{2}} & 0 & 0 & 0 \\ 0 & 1+e^{-\frac{\sigma^2}{2}} & -2e^{-\frac{\sigma^2}{2}} & 0 \\ 0 & -2e^{-\frac{\sigma^2}{2}} & 1+e^{-\frac{\sigma^2}{2}} & 0 \\ 0 & 0 & 0 & 1-e^{-\frac{\sigma^2}{2}} \end{pmatrix}, \tag{29}$$

and by comparing Eqs.(22) and (29) we find the relation

$$\lambda_B t = \frac{\sigma^2}{2} \tag{30}$$

between the decoherence parameter $\lambda_B$ and the deviation $\sigma$ of the Gaussian distribution.

*Experimental test.* Our decoherence modes A and B can be tested experimentally in the following way. The incoming polarized neutron, prepared after the beam splitter and spin flipper in a Bell singlet state, is subjected to magnetic fields with a certain Gaussian

variation $\sigma$ in both paths of the interferometer (see Fig.2 for mode A and Fig.3 for mode B). Due to relation (27) for mode A and (30) for mode B the value of the decoherence parameter $\lambda$ – the "dephasing" due to the variation of the magnetic fields – is adjusted. The time $t$ corresponds to the duration the neutron remains in the interferometer, more precisely, within the magnetic fields and remains constant. The individual density matrix elements are measured experimentally via quantum state tomography and have to be compared with the corresponding theoretical expressions (21) and (22). By varying $\sigma$, which means varying $\lambda$, one can nicely examine the specific exponential decrease of the decoherence modes A and B.

## V. CONNECTION TO THE KRAUS OPERATOR DECOMPOSITION

In the following section we present a connection to the Kraus operator decomposition. According to the theory of decoherence [1, 2, 3] the non-unitary evolution of the system can be described by Kraus operators. We want to demonstrate that by a simple experiment within neutron interferometry. We can check whether the theoretically predicted Kraus operators correspond to the implemented decoherence modes discussed in Sect.IV.

### A. Kraus operator decomposition

The completely positive time evolution generated by the Liouville – von Neumann master equation (1) together with the Lindblad form of the dissipator (2) can also be represented by a dynamical map expressed in the Kraus operator decomposition [2, 23]

$$\rho(0) \mapsto \rho(t) = \sum_k M_k \rho(0) M_k^\dagger \ , \tag{31}$$

where the Kraus operators $M_k$ fulfil $\sum_k M_k^\dagger M_k = \mathbb{1}$. The first approach corresponds to a continuous time-dependence of the state whereas the second one treats decoherence via discrete state changes. Both views are equivalent and a correspondence between Lindblad generators $A_k$ and Kraus operators $M_k$ exists for small $\delta t$ (see e.g. Ref.[24])

$$\begin{aligned} M_0 &= \mathbb{1} - (iH + \frac{1}{2}\sum A_k^\dagger A_k)\delta t \\ M_k &= \sqrt{\delta t}\, A_k \ . \end{aligned} \tag{32}$$

Clearly, the Kraus operators are not uniquely determined by Eq.(31) and allow for a unitary transformation.

### B. Mode A

For the Hilbert space we are using, $\mathcal{H}_{\text{spin}} \otimes \mathcal{H}_{\text{path}}$, where entanglement occurs between spin and spatial degrees of freedom, mode A represents a kind of phase flip channel [2, 24]

which destroys the coherence of the system. In this case the Kraus operators are given by

$$M_0 = \sqrt{1 - \frac{3w}{4}}\ \mathbb{1}^s \otimes \mathbb{1}^p \qquad M_1 = \sqrt{\frac{w}{4}}\ \mathbb{1}^s \otimes \sigma_z^p$$
$$M_2 = \sqrt{\frac{w}{4}}\ \sigma_z^s \otimes \mathbb{1}^p \qquad M_3 = \sqrt{\frac{w}{4}}\ \sigma_z^s \otimes \sigma_z^p\ , \tag{33}$$

where $w = \lambda t$ is the probability for the occurring decoherence. It leads for small $\delta t$ to the state $\rho(t)$, Eq.(6), which allows for a general initial condition.

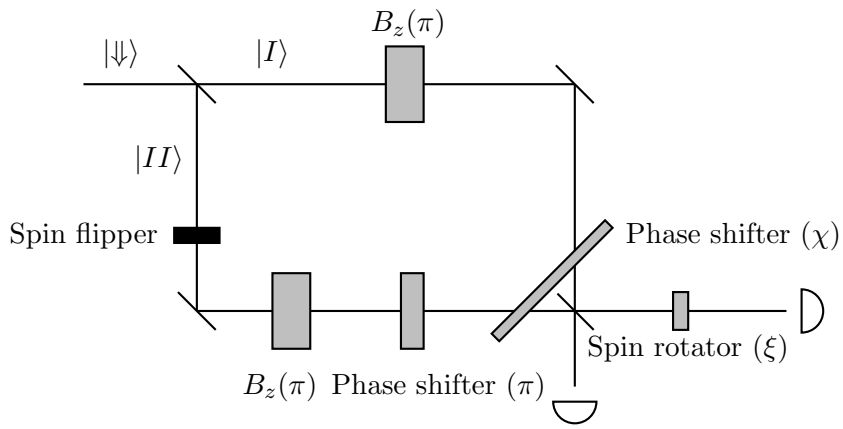


FIG. 4: Experimental setup for the realization of the Kraus operator $\sigma_z^s \otimes \sigma_z^p$ for mode A.

Experimentally the Kraus operators can be implemented in the interferometer in the following way. Incoming polarized neutrons are prepared as Bell singlet states and feel the effect caused by the Kraus operators, as shown in Fig.4 for the operator $M_3$. The identity operators $\mathbb{1}^s$ and $\mathbb{1}^p$ clearly do not change the spin and spatial degree of freedom. The operator $\sigma_z^s$ when acting on the spin state $|\Downarrow\rangle$ induces a phase shift of $\pi$. This phase shift difference between spin up and spin down can be implemented by a magnetic field in $z$-direction $B_z$ (modulo an overall phase shift). The operator $\sigma_z^p$ on the spatial subspace is realized by a phase shifter in the path $|\mathrm{II}\rangle$ which induces a fixed phase shift of $\pi$.

The states produced by the four Kraus operators are measured tomographically and the weighted sum according to (33) represents the state $\rho$, Eq.(21), of mode A.

### C. Mode B

Mode B is a combination of a bit flip channel and a phase flip channel [2, 24]. The corresponding Kraus operators are

$$M_0 = \sqrt{1 - \frac{3w}{4}}\ \mathbb{1}^s \otimes \mathbb{1}^p \qquad M_1 = \sqrt{\frac{w}{4}}\ \mathbb{1}^s \otimes \sigma_z^p$$
$$M_2 = \sqrt{\frac{w}{4}}\ \sigma_x^s \otimes \mathbb{1}^p \qquad M_3 = \sqrt{\frac{w}{4}}\ \sigma_x^s \otimes \sigma_z^p\ , \tag{34}$$

and create for small $\delta t$ the state given by Eqs. (11), (12) and (13) ($w = \lambda t$) allowing for general initial conditions.

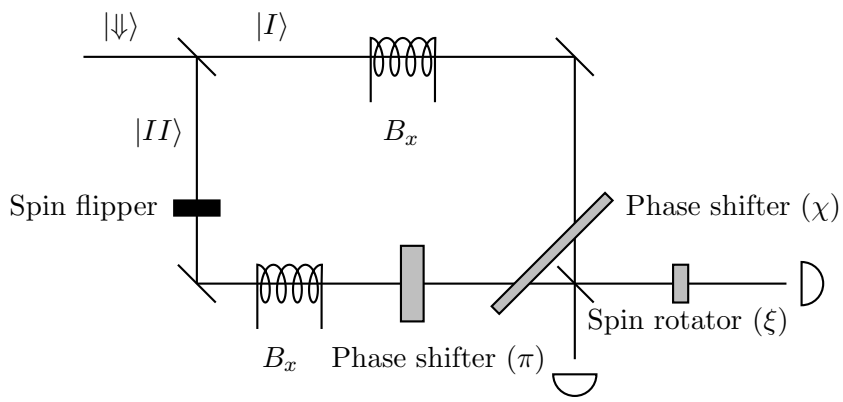


FIG. 5: Experimental setup for the realization of the Kraus operator $\sigma_x^s \otimes \sigma_z^p$ for mode B.

The Kraus operator for the spatial part $\sigma_z^p$ is the same as for mode A, inducing a phase shift of $\pi$. The difference to mode A lies in the $\sigma_x^s$ operator for the spin part. It can be realized by two magnetic fields $B_x$ in both arms pointing in the $x$-direction, which cause a spin flip, see Fig.5.

Again, the weighted sum of the measured states produced by the Kraus operators according to (34) leads to the state (22) of mode B.

## VI. SUMMARY AND CONCLUSION

We have considered the Liouville – von Neumann equation where decoherence is implemented by the dissipator in Lindblad form. We study two kinds of decoherence modes where the Lindblad generators are given by different projection operators: decoherence in the eigenbasis of the Hamiltonian, mode A, and decoherence in a rotated basis, mode B. The two modes are analyzed in detail for Bell diagonal states, where it turns out that in mode B the state gets more mixed and the entanglement decreases faster than in mode A. The Bell singlet state $|\Psi_4\rangle$ gets separable at finite $\lambda t = \ln 3$ in mode B whereas in mode A the state remains still entangled at that point by an amount of 33%.

The realization of the proposed decoherence modes uses the bipartite Hilbert space construction of neutron interferometry where entanglement for single neutrons occurs between an internal (spin) and an external (path) degree of freedom.

We create decoherence via magnetic fields in the interferometer and find that the decoherence parameter $\lambda$ is determined by the deviation $\sigma$ of the fluctuating fields, Eqs. (27) and (30). This allows an experimental control of the implemented decoherence in each mode. The strength of decoherence does not depend on the actual rotation parameter $\alpha$ of the magnetic field but only on the width of the Gaussian distribution.

Measuring experimentally the matrix elements of a state via state tomography and varying $\sigma$ we examine the time evolution of the state according to mode A and mode B, Eqs. (21) and (22).

In addition we can test experimentally the validity of the Kraus operator decomposition which alternatively describes the completely positive time evolution. The Kraus operators are constructed for each mode and realized within neutron interferometry.

## Acknowledgments

The authors want to thank Stefan Filipp, Jürgen Klepp and Helmut Rauch for helpful discussions.

This research has been supported by the EU project EURIDICE EEC-TMR program HPRN-CT-2002-00311 (R.A.B., K.D.), the University of Vienna (Förderungsstipendium of K.D.) and the FWF-project P17803-N02 of the Austrian Science Foundation (Y.H.).

---

[1] H.-P. Breuer and F. Petruccione, *The theory of open quantum systems* (Oxford University Press, New York, 2002).

[2] M. Nielsen and I. Chuang, *Quantum computation and quantum information* (Cambridge University Press, Cambridge, 2000).

[3] D. Giulini, E. Joos, C. Kiefer, J. Kupsch, I.-O. Stamatescu, and H.D. Zeh, *Decoherence and the Appearance of a Classical World in Quantum Theory* (Springer Verlag, Berlin, 1996).

[4] W. Zurek, Physics Today **44**, 36 (1991).

[5] G. Lindblad, Comm. Math. Phys. **48**, 119 (1976).

[6] V. Gorini, A. Kossakowski, and E. Sudarshan, J. Math. Phys. **17**, 821 (1976).

[7] R.A. Bertlmann and W. Grimus, Phys. Lett. A **300**, 107 (2002).

[8] R.A. Bertlmann, K. Durstberger, and B.C. Hiesmayr, Phys. Rev. A **68**, 012111 (2003).

[9] R.A. Bertlmann and W. Grimus, Phys. Rev. D **64**, 056004 (2001).

[10] D. Bouwmeester, A. Ekert, and A. Zeilinger, *The physics of quantum information: Quantum Cryptography, Quantum Teleportation, Quantum Computation* (Springer-Verlag, Berlin, 2000).

[11] B.C. Hiesmayr, Ph.D. thesis, University of Vienna, 2002.

[12] R.A. Bertlmann, *Entanglement, Bell inequalities and decoherence in particle physics*, Lecture Notes in Physics (Springer-Verlag, Berlin, 2005), quant-ph/0410028.

[13] S. Hill and W. Wootters, Phys. Rev. Lett. **78**, 5022 (1997).

[14] W. Wootters, Phys. Rev. Lett. **80**, 2245 (1998).

[15] W. Wootters, Quantum Information and Computation **1**, 27 (2001).

[16] T. Yu and J. Eberly, *Evolution and control of decoherence of "standard" mixed states*, quant-ph/0503089.

[17] H. Rauch and S. Werner, *Neutron Interferometry: Lessons in Experimental Quantum Mechanics* (Oxford University Press, Oxford, 2000).

[18] Y. Hasegawa, R. Loidl, G. Badurek, M. Baron, and H. Rauch, Nature **425**, 45 (2003).

[19] Y. Hasegawa, R. Loidl, G. Badurek, M. Baron, and H. Rauch, J. Opt. B: Quantum and Semiclass. Opt. **6**, 7 (2004).

[20] R.A. Bertlmann, K. Durstberger, Y. Hasegawa, and B.C. Hiesmayr, Phys. Rev. A **69**, 032112 (2004).

[21] Y. Hasegawa, R. Loidl, J. Klepp, S. Filipp, and H. Rauch, *Quantum state tomography of neutron's Bell-states*, to be published.

[22] D. James, P. Kwiat, W. Munro, and A. White, Phys. Rev. A **64**, 052312 (2001).

[23] K. Kraus, *States, Effects and Operations: Fundamental Notations of Quantum Theory* (Springer Verlag, Berlin, 1983).

[24] J. Preskill, *Lecuture notes*, http://theory.caltech.edu/people/preskill/ph229/.